Mon. Not. R. astr. Soc. (1984) **209**, 895–904

Frequency shifts and line broadening of radiation from rotating neutron stars

R. C. Kapoor and B. Datta *Indian Institute of Astrophysics, Bangalore 560034, India*

Accepted 1984 February 6. Received 1984 January 25; in original form 1983 November 23

Summary. The frequency shifts and line broadening of radiation from the surface of rapidly rotating neutron stars are calculated using a rotationally perturbed interior spherical metric and a representative choice of the equation of state for neutron star matter. The effect of rotation on the surface redshift and Doppler broadening are found to be substantial for rotation close to the secular instability limit, relevant for fast pulsars. If gamma-ray line emission originates from the surface of such pulsars, the results presented here can be used to constrain the validity of the equation of state of matter at high densities.

1 Introduction

A study of redshifts of radiation from neutron stars is of astrophysical significance because the interpretation of observed gamma-ray line as redshifted electron–positron annihilation line emitted from the star's surface provides an insight into the neutron star structure and can constrain equations of state for matter at high densities (Ramaty, Borner & Cohen 1973).

For all the neutron stars identified up until recently, the effect of rotation on the structure is known to be negligible, and so, it is adequate to use the spherically symmetric Schwarzchild metric in determining the structure, and hence the redshift factor and the gravitational line broadening (due to variation of potential over small regions near the star's surface). Substantial rotation will alter the structure as well as induce the relativistic effect of dragging of inertial frames, which will deform photon trajectories and give rise to an asymmetry in the Doppler-broadened spectral line. The purpose of this paper is to investigate such effects with a view of applicability to the recently discovered fast pulsar PSR 1937 + 214 (Backer *et al.* 1982) and pulsars of this class.

The Kerr solution, the rotational analog to the Schwarzchild space-time, does not have a corresponding appropriate interior solution amenable to a straightforward theoretical treatment. It is, however, adequate to use a rotationally perturbed interior spherical metric to take rotational effects into account.

2 Rotating neutron star model

The effect of rotation on the structure of the neutron star (assuming the star to be homogeneous and in rigid rotation) is to produce both spherical and quadrupole deforma-

tions. For a fixed central density, the fractional changes in the (gravitational) mass ($\delta M/M$) and radius ($\delta R/R$) due to spherical deformation are proportional to Ω^2 (Ω = angular velocity), and can be obtained from a knowledge of the radial distributions of the mass and pressure perturbation factors. The non-rotating mass M and radius R are obtained by integrating the relativistic equations for hydrostatic equilibrium (see e.g. Arnett & Bowers 1977).

The mass perturbation factor $m_0(r)$ and the pressure perturbation factor $P_0(r)$ corresponding to spherical deformation are calculated using the prescription of Hartle & Thorne (1968), according to which the deformations δM and δR are given by ($c = 1 = G$)

$$\delta M = m_0(R) + J^2/R^3 \tag{1}$$

$$\delta R = -\left.\frac{P_0(\rho + P)}{dP/dr}\right|_{r=R} \tag{2}$$

where J and R are respectively the angular momentum and radius of the star and $P(r)$ and $\rho(r)$ are the pressure and total mass–energy density at the point r. The metric (signature $+---$) that describes the perturbed geometry and that matches at the surface to an exterior metric is

$$ds^2 = g_{\alpha\beta}dx^\alpha dx^\beta \qquad (\alpha, \beta = 0, 1, 2, 3)$$
$$= e^{2\nu}dt^2 - e^{2\psi}(d\phi - \omega dt)^2 - e^{2\mu}d\theta^2 - e^{2\lambda}dr^2 + O(\Omega^3/\Omega_c^3) \tag{3}$$

where the metric components correspond to the interior with

$$e^{2\nu} = e^{2\Phi}\{1 + 2(h_0 + h_2P_2)\} \tag{4}$$

$$e^{2\psi} = r^2\sin^2\theta\{1 + 2(v_2 - h_2)P_2\} \tag{5}$$

$$e^{2\mu} = r^2\{1 + 2(v_2 - h_2)P_2\} \tag{6}$$

$$e^{2\lambda} = \frac{1 + 2(m_0 + m_2P_2)/(r - 2m)}{(1 - 2m/r)} \tag{7}$$

so that

$$\begin{aligned} g_{00} &= e^{2\nu} - e^{2\psi}\omega^2 \\ g_{11} &= -e^{2\lambda} \\ g_{22} &= -e^{2\mu} \\ g_{33} &= -e^{2\psi} \\ g_{03} &= \omega e^{2\psi} \end{aligned} \tag{8}$$

the rest of the components of $g_{\alpha\beta}$ being zero. Here Φ is the gravitational potential, P_2 is the Legendre polynomial of order 2, ω is the angular velocity of the cumulative dragging and h_0, h_2, m_0, m_2, v_2 are all functions of r that are proportional to Ω^2.

Fast pulsars such as PSR 1937 + 214 are close to the onset of rotational instability. So, for the sake of numerical estimates, we take rotating neutron star configurations to correspond to the angular velocity at the secular instability limit (Ω_s), using the above formalism. This can be justified, since $\Omega_s \simeq 0.5\,\Omega_c$ where $\Omega_c \equiv (M/R^3)^{1/2}$ is an upper bound on those angular velocities for which the Hartle & Thorne prescription is valid.

The calculations of Datta & Ray (1983) show that for realistic equations of state and stable configurations, the spherical deformation terms for mass and radius (characterized

by the subscript (0) do not exceed 10 and 5 per cent respectively for the star rotating at the secular instability limit. Therefore, we neglect the contributions due to the quadrupole terms [characterized by the subscript (2)] which will not be significant. The external solution has, in general, a complicated form. Since we are interested only in the surface radiation, equation (3) suffices for our purpose.

3 Frequency shifts

In calculating frequency shifts we use the geometrical optics approximation that photons are zero rest mass particles which follow null geodesics, and neglect the back scattering caused by the presence of the space-time curvature. The general expression for the frequency shift is given by (Schrödinger 1956):

$$1+z=\frac{\lambda_{\rm obs}}{\lambda_{\rm em}}=\frac{\nu_0}{\nu}=\frac{(\boldsymbol{u}\cdot\boldsymbol{p})_{\rm source}}{(\boldsymbol{u}\cdot\boldsymbol{p})_{\rm obs}} \tag{9}$$

where $(u^\alpha)_{\rm source}=dx^\alpha/ds=4-$velocity of the source, $(u^\alpha)_{\rm obs}=4-$velocity of a distant observer $=(1,\ 0,\ 0,\ 0)$ and $p^\alpha=$direction of null ray at position r. Our notation is: $x^0=t$, $x^1=r$, $x^2=\theta$, $x^3=\phi$.

The angular velocity of the star is

$$\Omega=u^3/u^0. \tag{10}$$

The photon impact parameter (q) can be defined in terms of the constants of motion

$$q=p_3/p_0=-h/\gamma \tag{11}$$

where h is the orbital angular momentum and γ is the energy as measured at infinity. Equation (9) then becomes

$$\begin{aligned}1+z&=\frac{p_0u^0(1+\Omega q)|_r}{p_0u^0|_\alpha}\\&=u^0(1+\Omega q)|_r.\end{aligned} \tag{12}$$

For a material particle for which $dr/ds=0$ (which refers to surface of constant r), the time-component of its 4-velocity is, from metric equation (3)

$$u^0=\frac{dt}{ds}=\frac{1}{e^\nu(1-v_{\rm s}^2)^{1/2}} \tag{13}$$

where

$$v_{\rm s}=e^{\psi-\nu}(\Omega-\omega).$$

The general expression for the frequency shift then becomes

$$1+z=\frac{1+\Omega q}{e^\nu(1-v_{\rm s}^2)^{1/2}} \tag{14}$$

which, within the approximations used to obtain the structure of the star, can be written as

$$1+z=(1+\Omega q)\{e^{2\Phi}(1+2h_0)-r^2\sin^2\theta_{\rm s}\,\bar{\omega}^2\}^{-1/2} \tag{15}$$

where $\bar{\omega}=\Omega-\omega$. The surface red shift of a rotating star corresponds to $q=0$, and is given by

$$1+z_{\rm R}=\{e^{2\Phi}(1+2h_0)-r^2\sin^2\theta_{\rm s}\,\bar{\omega}^2\}^{-1/2}_{r=R}. \tag{16}$$

Here, θ_s the polar angle of emission is that made by the line-of-sight through the centre of the star with respect to the axis of rotation, such that $\theta_s = 0$ corresponds to looking along the pole and $\theta_s = \pi/2$ along the equator. We have taken θ_s to be identical to the angle of inclination according to the distant observer since the polar bending in the trajectory of a photon propagating in the perturbed exterior Schwarzchild space-time would be small compared to the azimuthal bending. Interestingly, our results show that calculated redshifts, etc., are relatively insensitive to large variations in θ_s.

4 Spectral line broadening

A photon emitted at a certain $\theta = \theta_s$ would be bent in the azimuthal direction and dragged due to space-time curvature. If the emission is localized and isotropic, then there always exists a point on the trajectory of the emitter on the surface of the neutron star from where such a photon will be received by a distant observer. For isotropic emission, whether localized or spread over the surface, line broadening caused by rotation can be evaluated from equation (14).

The gravitational field produced by the rotating mass possesses two Killing vectors: the stationary Killing vector

$$\xi^a = \delta^a_0 \tag{17}$$

and the space-like (rotational) Killing vector

$$\eta^a = \delta^a_3 \tag{18}$$

where δ^i_j is the Kronecker delta function. As a consequence of Killing's equations, the scalars

$$\xi^a p_a = \gamma \tag{19}$$

and

$$\eta^a p_a = -h \tag{20}$$

will be constants along the geodesics (Misner, Thorne & Wheeler 1973, MTW). These correspond to the equations of motion for photons and can be written as

$$\xi^a p_a = p_0 = g_{0a}p^a = g_{00}p^0 + g_{03}p^3 = \gamma \tag{21}$$

$$\eta^a p_a = p_3 = g_{3a}p^a = g_{03}p^0 + g_{33}p^3 = -h. \tag{22}$$

If Γ is an affine parameter, then for $ds^2 = 0$, equation (3) can be rewritten as

$$e^{2(\psi-\nu)}(X-\omega)^2 + e^{2(\lambda-\nu)}\left(\frac{dr/d\Gamma}{dt/d\Gamma}\right)^2 = 1 \tag{23}$$

which corresponds to a null ray. In equation (23) the quantity X is

$$X = p^3/p^0 = \frac{d\phi/d\Gamma}{dt/d\Gamma}. \tag{24}$$

We first evaluate the impact parameter in the frame of reference of a locally non-rotating observer, that is, one having (r, θ) fixed and rotating with a coordinate angular velocity $d\phi/dt = \omega$. For this observer, the two physical components V_r and V_ϕ of the photon velocity with respect to the proper frame of reference of the observer can be written as (see e.g. Kapoor 1981)

$$V_r = e^{\lambda-\nu}\frac{dr/d\Gamma}{dt/d\Gamma} \tag{25}$$

and

$$V_\phi = e^{\psi-\nu}(x-\omega). \tag{26}$$

Since $V_r^2 + V_\phi^2 = 1$, we can write

$$V_r = \cos\delta'; \qquad V_\phi = \sin\delta' \tag{27}$$

where δ' is the azimuthal angle at which the photon is emitted with respect to the radius vector of the source through the origin of the system of coordinates as seen by the non-rotating observer, and it increases in the direction opposite to that of motion of the source. For a radially outgoing photon, $\delta' = 0$, and for a tangential photon emitted in the forward direction, $\delta' = 3\pi/2$.

The expression for the impact parameter is obtained by using equations (21), (22) and (26). It is given by

$$q = \left.\frac{e^{\psi-\nu}\sin\delta'}{1+\omega e^{\psi-\nu}\sin\delta'}\right|_{r=R}. \tag{28}$$

For the non-rotating observer, $q = 0$ for $\delta' = 0$ or π. If we define δ as the azimuthal angle of emission with respect to the radius vector of the source through the origin, as seen in the local rest frame of the star, a Lorentz transformation to the source through the relation

$$\sin\delta = \frac{\sin\delta' - v_s}{1 - v_s\sin\delta'} \tag{29}$$

gives

$$q = \left.\frac{e^{\psi-\nu}(v_s+\sin\delta)}{1+e^{\psi-\nu}(\omega v_s+\Omega\sin\delta)}\right|_{r=R} \tag{30}$$

v_s being the velocity of the source according tothe non-rotating observer. Like δ', δ increases in the direction opposite to that of the motion of the source.

It can be seen from equation (30) that the $q = 0$ photon in the emitter's frame of reference has

$$\delta \equiv \delta_0 = \sin^{-1}(-v_s). \tag{31}$$

In the Schwarzchild case (Kapoor 1981), and, in the rotating case, in the frame of reference of locally non-rotating observer $\delta'_0 = 0$.

The general relativistic expression for the spectral line broadening can be calculated from a knowledge of the maximum and minimum values of the impact parameter (q_{max}, q_{min}). The quantity q_{max} (which is positive) corresponds to a photon emitted tangentially backwards, that is, from that equatorial limb of the star that moves away from the distant observer. The quantity q_{min} (which is negative) corresponds to a photon emitted tangentially forwards, that is, from that limb of the star that moves towards the observer. Because of the dragging of inertial frames,

$$q_{max} \neq -q_{min},$$

unlike the Newtonian or the Schwarzchild field case.

If E_{em} is the energy of the emitted photon, we can write the general relativistic line broadening due to rotation as

$$W = E_{em}\left\{\frac{1}{1+z(q_{min})} - \frac{1}{1+z(q_{max})}\right\}. \tag{32}$$

The maximum and minimum values of W correspond respectively to $\theta_s = \pi/2$ and 0.

The line centre corresponds to $q = 0$, which is redshifted by an amount given by equation (16). The effect of dragging of inertial frames is to position the broadened spectral line asymmetrically with respect to the line centre.

We next consider the intensity ratio near the wings of the broadened spectral line. The standard procedure, in dealing with the propagation of zero rest mass particles through space-time, is to discuss the specific intensity (I) rather than the number of particles in a region of phase space. The Liouville's theorem relates the observed I_ν and the emitted monochromatic specific intensity I_{ν_0} through the equation

$$I_\nu = I_{\nu_0}(\nu/\nu_0)^3. \tag{33}$$

Therefore, the ratio of intensities near the wings of the broadened line is

$$\frac{I_{\text{blue}}}{I_{\text{red}}} = \left\{\frac{1+z(q_{\max})}{1+z(q_{\min})}\right\}^3. \tag{34}$$

5 Choice of the equation of state (EOS)

The structure of neutron stars depends sensitively on the EOS at high densities, especially around $\rho \sim 10^{15}$ g cm^{-3}. We have chosen the following five EOS based on representative models: (1) Reid-Pandharipande (RP) model, (2) Bethe-Johnson (BJ) model I, (3) the tensor interaction (TI) model (for a detailed discussion on these three models see Pandharipande, Pines & Smith 1976), (4) Canuto-Datta-Kalman (CDK) model which includes the short range attraction due to nucleon–nucleon f^0 meson exchange ($f^2 = 2.91$ case) Canuto, Datta & Kalman (1978) and (5) Friedman-Pandharipande (FP) model, which is based on an improved nuclear Hamiltonian that fits adequately 2-nucleon scattering data and known nuclear matter properties (Friedman & Pandharipande 1981). The details of the rotating neutron star models for these EOS have been reported in Datta & Ray (1983).

6 Results and Discussion

Analysis of available binary pulsar data are consistent with a neutron star mass in the range $(1.4 \pm 0.2)M_\odot$ (Joss & Rappaport 1984). We have, therefore taken this as representative neutron star mass for the purpose of illustrating the effect of rotation on the frequency shift and line broadening.

In Table 1 we have listed the parameters regarding the structure of neutron stars rotating at the secular instability limit (Datta & Ray 1983) that are relevant for the calculations of the surface redshift and line broadening. Fig. 1 shows the surface redshift factor $(1 + z_R)$ (i.e. $q = 0$ case) for the rotational case as a function of the angle θ_s for various EOS. For larger θ_s the redshift tends to increase, which is a consequence of the Doppler effect. The

Table 1. The bulk properties of neutron stars rotating at the secular instability limit (see text).

EOS	$M/M_\odot$	$\frac{\delta M}{M_\odot}$	R (cm)	J (g cm^2 s^{-1})	$\bar{\omega}(R)$ (s^{-1})	$\bar{e}^{\Phi}(R)$
RP	1.285	0.098	1.002×10^6	6.084×10^{48}	5.859×10^3	1.268
FP	1.308	0.108	1.087×10^6	6.492×10^{48}	5.285×10^3	1.245
CDK	1.305	0.118	1.141×10^6	6.675×10^{48}	4.939×10^3	1.229
BJ	1.301	0.098	1.281×10^6	6.105×10^{48}	4.274×10^3	1.195
TI	1.270	0.120	1.629×10^6	6.636×10^{48}	3.015×10^3	1.140

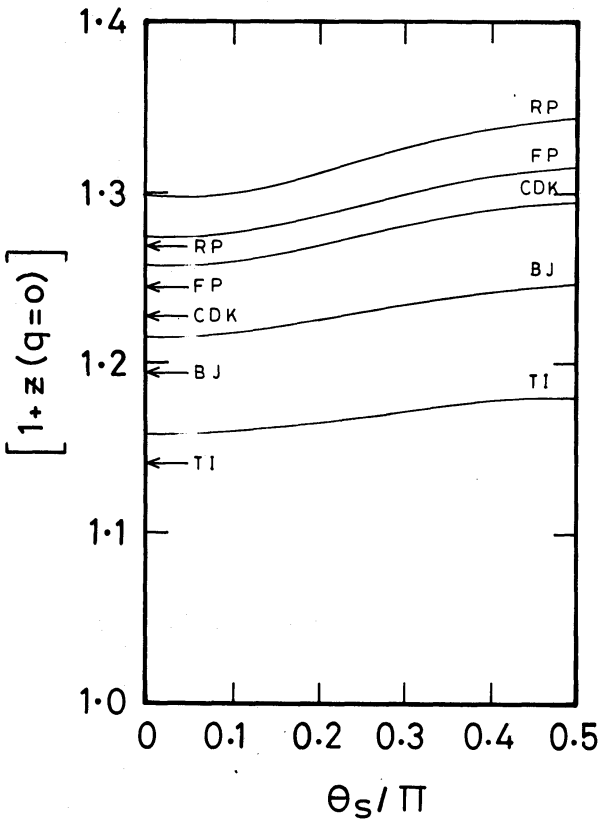

Figure 1. Surface redshift factor versus polar angle of emission θ_s for various equations of state. Arrows marked on the vertical scale are the corresponding Schwarzchild redshift factors: $(1-2M/R)^{-1/2}$.

corresponding Schwarzchild redshift factors $(1+z_s)$ are marked by arrows on the vertical scale. Generally speaking, the rotational surface redshifts are found to exceed the corresponding Schwarzchild values by ~12 per cent for $\theta_s = 0$ and ~27 per cent for $\theta_s = \pi/2$. It may be stressed that $(1+z_R)$ differs from $(1+z_s)$ even at $\theta_s = 0$, signifying the contribution of rotation.

The redshift factor for $q = 0$ is seen to have the following characteristics. For a given θ_s, as $|\delta|$ increases from 0 to $\pi/2$, $(1+z)$ has an increasing trend for the case of backward emission ($\delta > 0$) and a decreasing trend for forward emission ($\delta < 0$). This is again due to Doppler effect which is appreciable even for θ_s as small as 10°. As θ_s increases, the above trend gets comparatively steeper for all EOS in a consistent manner. A switch-over from redshift to blueshift for forward emission takes place when $\theta_s \gtrsim \pi/4$. In general, the switch-over emission angle δ_s is found to lie in the range $-\pi/3 < \delta_s < -\pi/2$. For the TI model, however, the switch-over occurs for $\delta_s \simeq -90°$ at $\theta_s = \pi/4$. As θ_s increases, δ_s tends to be pushed away from $-\pi/2$ towards 0. The blueshift (when it comes about) occurs earliest for the TI EOS. The amount of blueshift increases as one goes from the RP model to TI model (in the order shown in Table 1), and for any particular EOS, it increases as $\theta_s \to \pi/2$. These features are illustrated in Figs 2–4. The dotted line in each of these figures is the angle $\delta = \delta_0$ for which the impact parameter is zero; the corresponding redshifts are surface redshifts. A comparison of Figs 2–4 shows that $|\delta_0|$ increases as θ_s increases.

In Fig. 5, we have plotted the line width W as a function of θ_s, where we have chosen the e^+e^- annihilation line (0.511 MeV) for the purpose of illustration. The calculated line widths for all EOS are quite substantial particularly for $\theta_s \gtrsim \pi/4$. Fig. 6 shows the ratio of intensities at the wings of the broadened line as a function of θ_s. It is maximum at $\theta_s = \pi/2$,

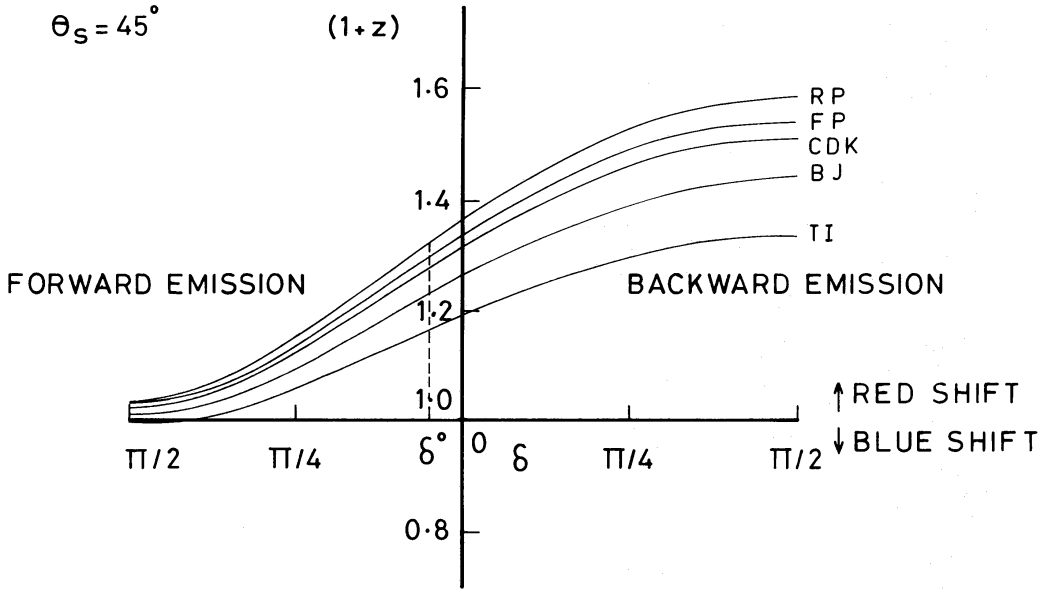

Figure 2. Redshift factor as a function of azimuthal emission angle δ for $\theta_s = 45°$. The dotted line corresponds to zero impact parameter.

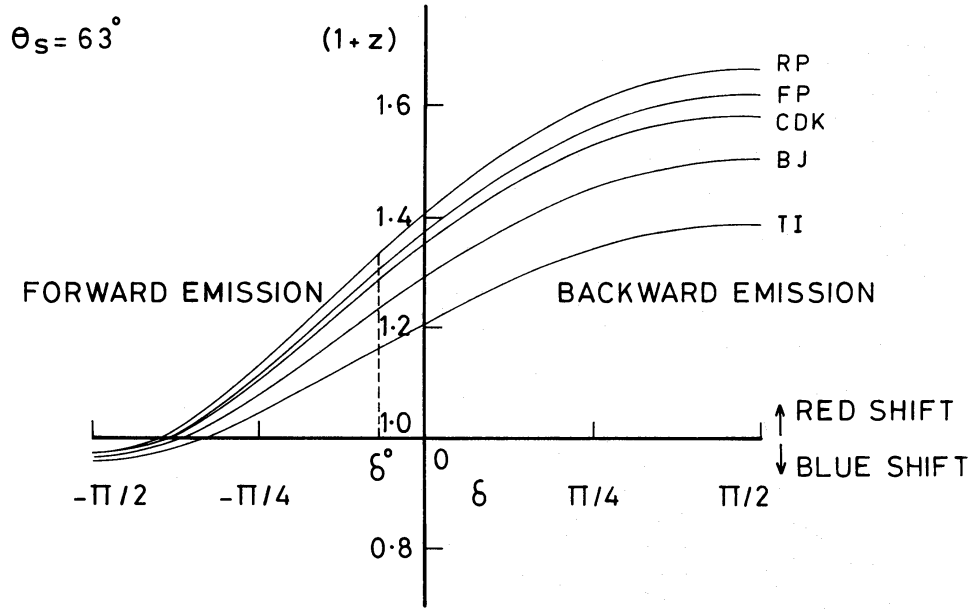

Figure 3. Redshift factor as a function of azimuthal angle δ for $\theta_s = 63°$.

and the largest value (~ 6) is suggested by the RP model. From equation (34), it follows that as the angular velocity gets larger, the asymmetry in the line profile becomes progressively substantial. Furthermore, for large rotation, as has been considered here, the blue end of the line will be conspicuous, suggesting more of the occurrence of a blueshifted line emission rather than a mere broadened one. These features are general, and will be valid for any other line emission, differing from each other only in the numerical magnitudes for the line width.

To summarize, in this paper we have calculated the surface redshift of neutron stars having substantial rotation (on the verge of secular instability), using a representative set of equations of state and a rotationally perturbed form of the interior spherical metric. The general relativistic formalism used here is exact to the extent that the geometric optics

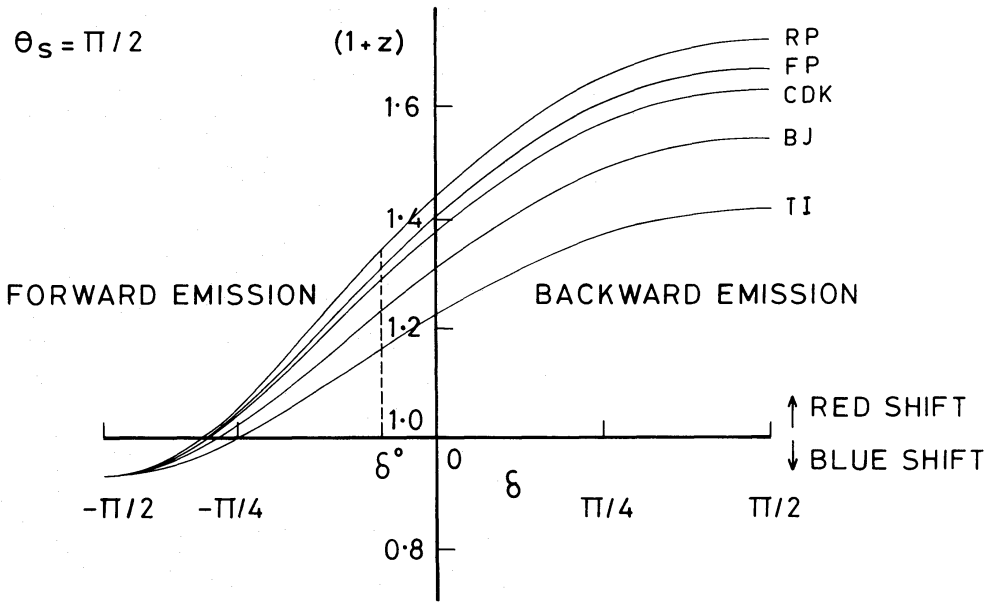

Figure 4. Redshift factor as a function of azimuthal angle δ for $\theta_s = 90°$.

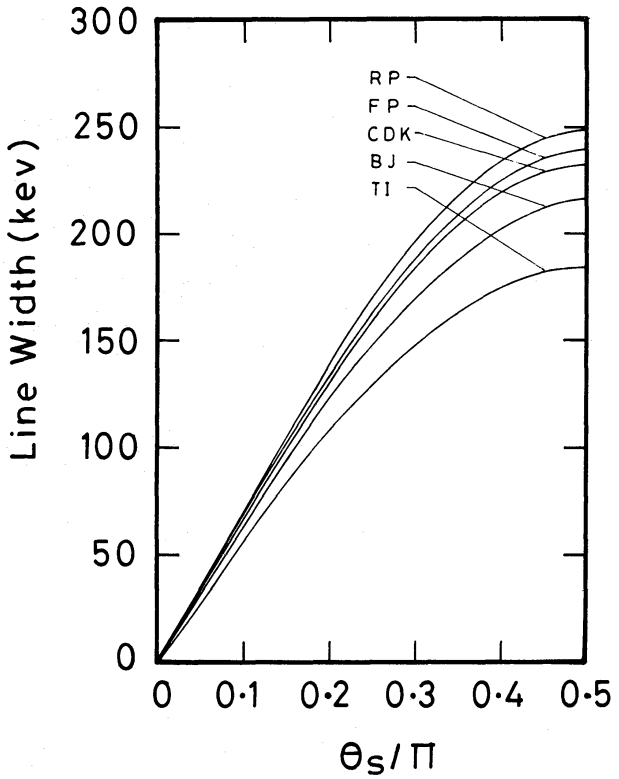

Figure 5. Line width as a function of polar angle of emission θ_s for various equations of state.

approximation is valid and the quadrupole and higher order terms in the metric are negligible. The calculated surface redshifts, Doppler broadening and the ratio of intensities at the edges of the broadened line are found to be substantial. The relativistic effect of dragging of inertial frames is also noticeable, resulting in a broadening which is asymmetric with respect to the line centre, which is already redshifted with respect to the rest wavelength. The equations of state, RP through TI as in Table 1, are arranged approximately

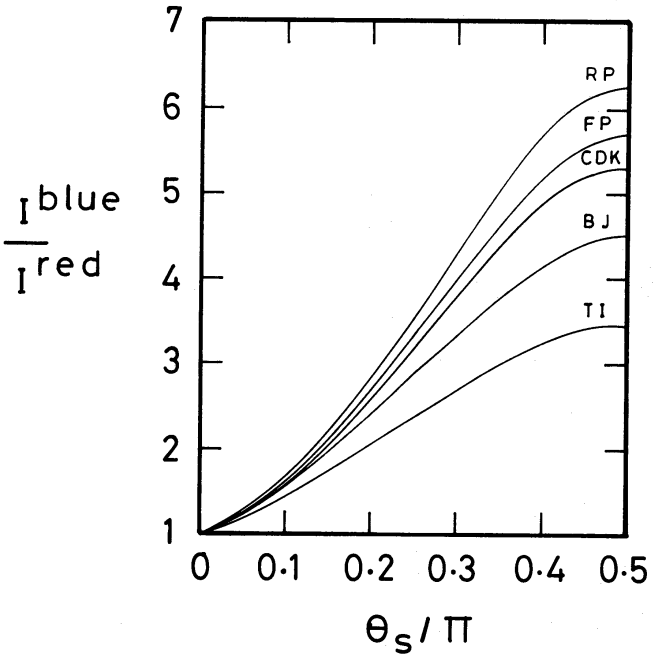

Figure 6. Ratio of intensities at the edges of a Doppler broadened spectral line versus polar angle of emission θ_s for various equations of state.

in the increasing order of 'stiffness', and the various figures indicate a behaviour of the calculated parameters that shows a one to one correspondence with 'stiffness' or equivalently the adiabatic index.

The emission of gamma-ray line from the surfaces of fast pulsars (such as PSR 1937+214) has not been established yet. Should such lines be discovered, the results presented here provide a new and interesting handle towards constraining the validity of equations of state proposed for neutron star matter. A large intensity ratio, if actually observed, would indicate that emission takes place at the surface, and the line emission is not predominantly gravitationally broadened, that is, the emission region is thin.

Acknowledgment

The authors thank Professors J. V. Narlikar, C. V. Vishveshwara and W. Kundt for helpful discussions.

References

Arnett, D. W. & Bowers, R. L., 1977. *Astrophys. J. Suppl.*, **33,** 415.
Backer, D. C., Kulkarni, S. R., Heiles, C., David, M. M. & Goss, W. M., 1982. *Nature,* **300,** 615.
Canuto, V., Datta, B. & Kalman, G., 1978. *Astrophys. J.*, **221,** 274 (CDK).
Datta, B. & Ray, A., 1983. *Mon. Not. R. astr. Soc.*, **204,** 75P.
Friedman, B. & Pandharipande, V. R., 1981. *Nucl. Phys.*, **A301,** 502 (FP).
Hartle, J. B. & Thorne, K. S., 1968. *Astrophys. J.*, **153,** 807.
Joss, P. & Rappaport, S., 1984. *Ann. Rev. Astr. Astrophys.*, in press.
Kapoor, R. C., 1981. *Bull. astr. Soc. Ind.*, **9,** 334.
Misner, C. W., Thorne, K. S. & Wheeler, J. A., 1973. *Gravitation*, p. 651, W. H. Freeman, San Fransisco (MTW).
Pandharipande, V. R., Pines, D. & Smith, R. A., 1975. *Nucl. Phys.*, **A237,** 507.
Ramaty, R., Borner, G. & Cohen, J. M., 1973. *Astrophys. J.*, **181,** 891.
Schrödinger, E., 1956. *Expanding Universe*, p. 49, Cambridge University Press.